Composition effect of the dental liquid mixture on droplet evaporation and deposition

Xiujie Li [1], Cheuk Ming Mak [1]*, Zhengtao Ai [2], Kuen Wai Ma [1], Hai Ming Wong [3]

1. *Department of Building Environment and Energy Engineering, The Hong Kong Polytechnic University, Hong Kong, China*
2. *Department of Building Environment and Energy, College of Civil Engineering, Hunan University, Changsha, 410082, China*
3. *Faculty of Dentistry, The University of Hong Kong, Hong Kong, China*

*Corresponding author. Email address: cheuk-ming.mak@polyu.edu.hk

Abstract:

The dilution effect of dental irrigants and the composition model of the liquid mixture have been typically overlooked in the transmission investigation of dental surgery. As the mass concentration of non-volatile components in droplets can determine the equilibrium size of dehydrated droplet nuclei and even the viral activity, the present study aims to numerically assess the evaporation characteristics of dental droplets in different compositions. The influence of organics in human saliva and adjuncts in dental irrigants can be revealed by the droplet spatial-temporal distribution, evaporation and deposition statistics. The results showed that the use of salt as an adjunct in dental irrigants could help enlarge the equilibrium size of droplet nuclei over 10 μm and increased the fraction of deposited droplets by 3%. The size range of

suspended particles exhibited an even 300% difference amongst the irrigant types. Droplets in the three-composition models have shorter evaporation times and larger deposition rates than the two-composition models. Therefore, the composition difference in the dental liquid mixtures should be further considered when conducting cross-infection assessments. The results can promote the development of dental guidelines by modifying the adjunct in dental irrigants to reduce the possibility of cross-infection.

Keywords: Droplet composition; Evaporation; Liquid mixture; Equilibrium size; Dental irrigants.

Introduction

A surge of interest has emerged in investigating the propagation patterns of droplet and aerosol particles in healthcare facilities. [1-3] This is because the activated viruses can be detected in the saliva and respiratory secretions during a respiratory infection. [4, 5] Three dominant transmission routes, airborne transmission, droplet transmission and direct contact, have been noticed in the surgery environments. [6, 7] Providing routine medical services in a healthy and comfortable environment is necessary for every individual. During dental atomization procedures, plenty of droplets and aerosol particles can be generated. The size distribution of the emitted particles can range from 5 to 250 μm. [8, 9] Several advanced experimental methods like high-speed cameras and luminescent tracers have been employed to identify the spatial-temporal distribution. [10-13] After being ejected from the treatment region, droplets gradually become

dehydrated until reaching the equilibrium size. Both the environmental conditions and droplet compositions can further affect the aforementioned size ratio. Overall, the droplet nuclei dehydrated from the large droplets can also be suspended in the air for a long time, and the cross-infection might occur once susceptible subjects have inhaled the virus-laden particles. Therefore, the evaporation and propagation characteristics of dental-emitted droplets should be accurately investigated, especially during the atomization procedures.

The final equilibrium size of respiratory droplets has been theoretically and experimentally investigated, which is about $20-40\%$ of the initial diameter.[14] Some researchers predicted the size of droplet nuclei to be 31% of the initial diameter. Droplets with high protein concentrations were different from those with low protein concentrations.[15-17] The final equilibrium size ratio for the low and high protein droplets were 0.19 and 0.41, respectively.[18] However, dental irrigants could dilute human saliva, increasing the volatile component (water) of emitted droplets. The continual employment of the aforementioned size ratio cannot be appropriate in dental surgery. Dental irrigants can help prevent injury of the pulp and soft tissues.[19] Many scholars assessed dental contaminations using the manikin phantom head, but they simplified the generation and composition of saliva mixture.[20-22] Overlooking the saliva composition might induce significant errors in evaluating the viral load of suspended particles and the exposure risks in dental surgery environments. Besides, the use of chemical agents in dental irrigants can change the mass ratio of droplet

components. The droplet generation, deposition and suspension characteristics can be further impacted. Some scholars indicated that adding the oxidant could affect the mean droplet size. The viscoelastic properties of liquid would change with the supply of different dental irrigants. [23, 24] However, they did not further specify the difference in evaporation and propagation properties of dental-emitted droplets. Therefore, the present study can contribute as the first research to quantitatively investigate the composition effect of the dental liquid mixture on droplet propagation and evaporation in the surgery environment.

High-resolution studies are warranted to resolve the droplet evaporation and propagation characteristics over a large space. [25, 26] Computational fluid dynamics (CFD) simulation has been widely employed to track particle dispersal in different scenarios. [27-30] However, limited numerical studies focused on specific dental clinics because of the difficulty in obtaining the initial boundary conditions. Some research even assumed that dental irrigants did not dilute human saliva. [31, 32] The evaporation characteristics of dental droplets were similar to those generated by sneezing and coughing. Besides, the respiratory droplets had been previously modelled as water or saline solutions. The organic components in droplets had been ignored. [7, 33] The aforementioned simplification can directly impact droplet suspension and deposition properties. [34] Therefore, the present study would employ the CFD to systematically investigate how the airflow interactions in dental clinics affect the propagation, evaporation and deposition patterns of dental droplets with different composition

models.

Dental irrigants employed in the procedures can change the viscoelastic properties of the liquid mixture, further affecting the droplet atomization, propagation and evaporation patterns in surgery environments. The present study analyzed the composition effect of dental droplets from their spatial-temporal distribution, evaporation time and deposition statistics. These factors can directly impact human exposure and cross-infection risks in dental environments. The results of the modification of chemical adjuncts in dental irrigants aimed to promote the development of source-control mitigation measures, update the dental guidelines and further provide crucial underpinnings for developing healthy and safe medical environments.

Numerical modelling

Computational domain and numerical setup

The computational domain for the dental surgery room is presented in Figure 1 (a), where the dimension aligns with our experimental chamber. The manikin models were obtained from the virtual manikin library. [35] The four-handed dentistry has been widely adopted in practice. The dental patient lay on the chair, and the dental professional sat next to the patient. A dental assistant stood by to prepare dental instruments. The dental surgery room was maintained at six air changes per hour (ACH) in the mixing ventilation. The air temperature and relative humidity were 23.5℃ and 50%, respectively. The boundary conditions were determined by our previous experimental

measurement. [9] Only the convective heat transfer was considered for the computational thermal manikin. The heat flux variation amongst the four different body segments (head, trunk, arms and legs) was also considered with a range from $23.5\ to\ 33\ W/m^2$. The non-slip adiabatic conditions were applied for the room wall and floor. As for the manikin breathing patterns, the periodic breathing airflow was also taken into consideration as shown in Figure 1 (c). The pulmonary ventilation rate of $0.36\ m^3/h$ was referred to human light activity condition. [36] The breathing of the dental professional was maintained as mouth inhalation/exhalation, while the breathing of the dental assistant was based on the nose patterns. The dental patient's nasal breathing was omitted to save computational resources. [32]

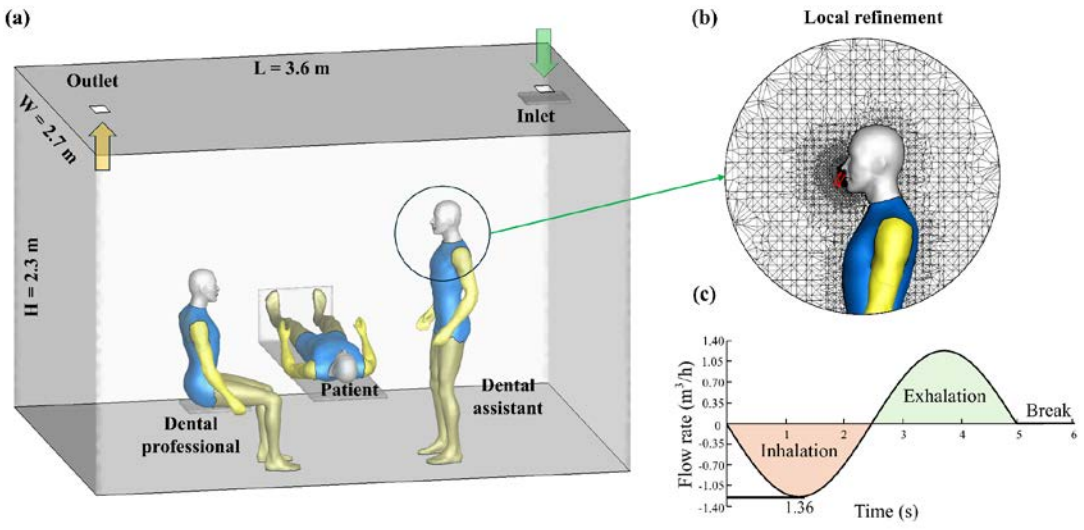

Figure 1 Computational domain and numerical setup: (a) The computational domain representing the dental surgery room; (b) Refined mesh near the manikins' breathing zone; (c) Sinusoidal breathing flow with the $6\ s$-breathing cycle

The computational domain was discretized by the unstructured mesh with

tetrahedral elements. Five prism layers were generated on the manikin skin surface to capture the temperature gradient and thermal plume accurately. The height of the first prism layer was set as $0.2\ mm$ to keep the $y+$ less than 1.0. The mesh was refined near the manikins' breathing zone to record the airflow fluctuation and particle dispersal details. The locally refined mesh was scaled up and presented in Figure 1 (b). The grid independence test was performed by generating the coarse (5.3 e^6 grids), medium (7.2 e^6 grids) and fine mesh (9.9 e^6grids). The velocity and temperature values from the measurement line $A-B$ were compared as shown in Figure 2. Considering the limited difference between the medium and fine mesh, the medium mesh of 7.27 e^6 grids was adopted to save computational costs.

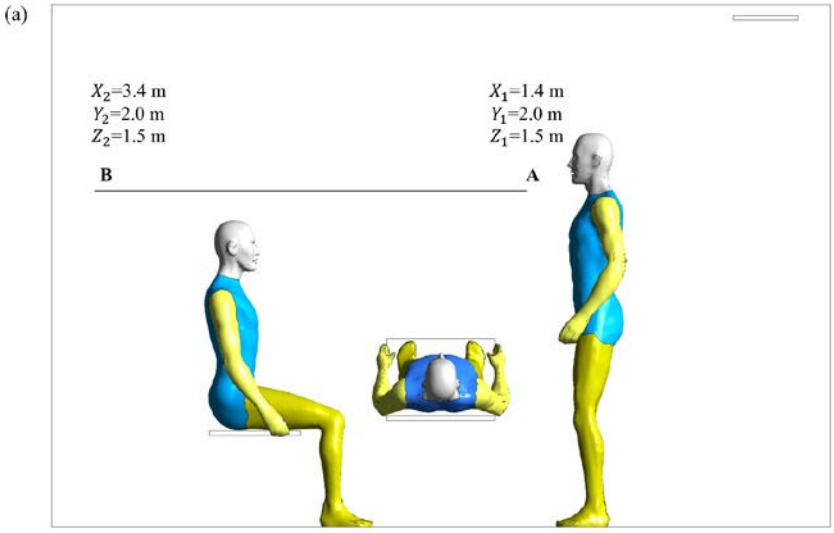

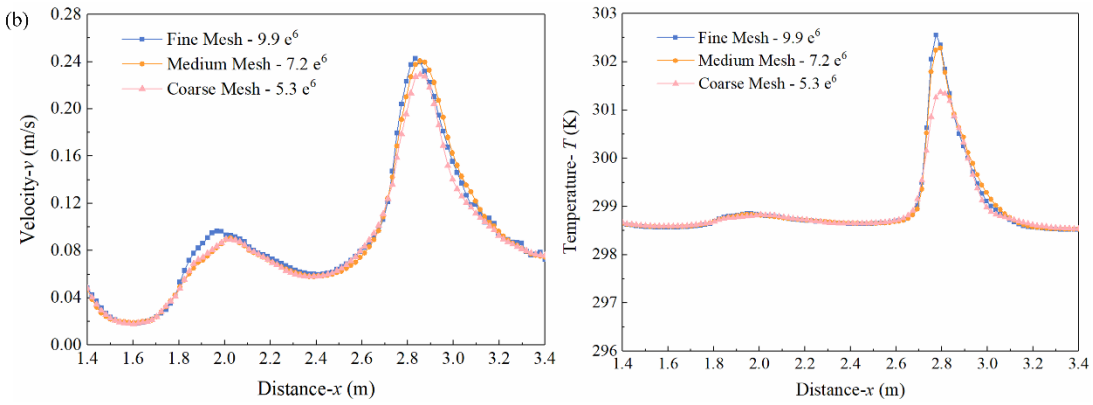

Figure 2 The grid independence test on the measurement line $A-B$ with the velocity magnitude and temperature

Boundary conditions

The airflow characteristics were simulated by the realizable $k-\varepsilon$ turbulence model. The model performance had been validated for the simulation of the airflow characteristics in indoor environments. [32] The pressure-velocity coupling was resolved by the SIMPLEC scheme, and the second-order upwind scheme was employed to discretize the momentum, energy, turbulent kinetic energy and dissipation rate. After the ambient ventilation flow and manikin thermal plume reached steady-state conditions, the modelling was then transferred to the transient model. The time step for the transient simulation was defined as $0.04\ s$. [37] Detailed numerical settings could be found in our previous research. [25, 38] As shown in Figure 3, the experimentally recorded diameter distribution was compared to the Rosin-Rammler distribution ($Y_d = e^{-(x/42.5)^{2.01}}$).

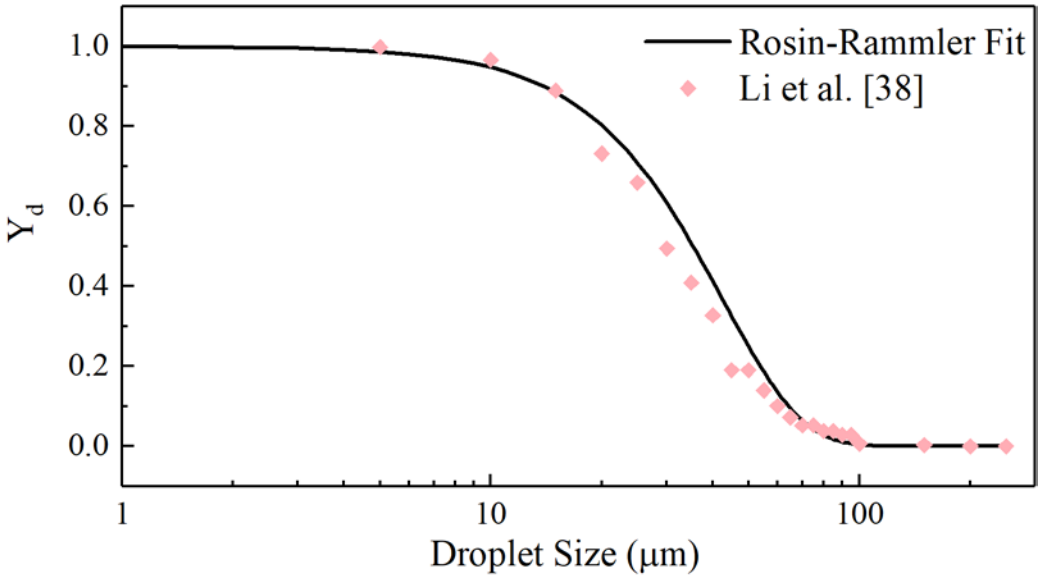

Figure 3 Diameter distribution of dental droplets compared to the Rosin-Rammler distribution in the discrete phase mode [38]

The dental droplets with a wide range size distribution from $5\,\mu m$ to $250\,\mu m$ were ejected from the oral cavity when conducting the ultrasonic scaling on the patient's central incisor (as shown in Figure 3). Besides, the droplet velocity and distribution cone angle were $2.6\,m/s$ and 30 degrees, respectively. [9] The mass flow rate was maintained at $0.001\,kg/s$. [38] The mean stimulated salivary flow rate was defined as 1.4 $ml/minute$. [39] The dental irrigants and human saliva were assumed to be well-mixed. To track the trajectories of emitted droplets, gravity, thermophoretic and Saffman lift forces were considered in the present study. The Fluent theory guide[40] had well-documented detailed force calculation equations. In addition, the discrete random walk model had also been adopted to track the turbulent dispersion of droplets.

As for the two-composition droplet models, the respiratory droplet was composed of water ($\rho = 998\ kg/m^3$, 98.2% of mass) and salt ($\rho = 2170\ kg/m^3$, 1.8% of mass).

[41] In the three-composition model, the respiratory droplet was composed of water ($\rho = 998\ kg/m^3$), glycerin ($\rho = 1260\ kg/m^3$) and salt ($\rho = 2170\ kg/m^3$). The mass fractions for the corresponding components were defined as 91.12%, 8%, and 0.88%, respectively. [42, 43] Besides, two types of dental irrigants, distilled water and 0.9% normal saline, were employed to dilute the human saliva. The water supply flow rate was 60 $ml/minute$ to keep in line with experimental conditions. Table 1 lists the six cases with different droplet composition models and irrigant types investigated in the present study.

Table 1 Different cases with the consideration of droplet composition models and dilution type of dental irrigants

Case	Type of droplet model	Type of dental irrigants
1	Two-composition model	No Dilution
2	Two-composition model	0.9% Normal saline
3	Two-composition model	Distilled water
4	Three-composition model	No Dilution
5	Three-composition model	0.9% Normal saline
6	Three-composition model	Distilled water

Model verifications

Droplet evaporation and airflow interaction around the human micro-environment can directly impact the dispersion characteristics of droplets and aerosols. Therefore,

two verifications for the continuous and discrete phase models were conducted in the present study. The first verification focused on the evaporation process of the two-composition respiratory droplet, and the second was on the human thermal plume under the buoyancy effect. The numerical settings of droplets in the verification were consistent with the current simulation. The comparison of the droplet evaporation process with the previous study was presented in Figure 4 (a). [41] The air temperature was kept at $25℃$. The droplet temperature was set as $37℃$, with a density of $1000\ kg/m^3$. The modelled evaporation process of respiratory droplets well reproduced the experimental result. Figure 4 (b) shows the second verification model of the manikin's thermal plume under the buoyancy effect. The simulated results were compared with prior particle image velocimetry (PIV) measurements. [44] Measurement error for the velocity was also considered. [9] The difference in the velocity magnitudes over 1.7 m (above the human shoulder) was noticed owing to the discrepancy in the shape of the manikin. Overall, satisfactory results were provided to predict the human thermal plume and evaporation process of respiratory droplets. These were the critical bases for accurately tracking the droplet evaporation and propagation patterns in the dental surgery environment.

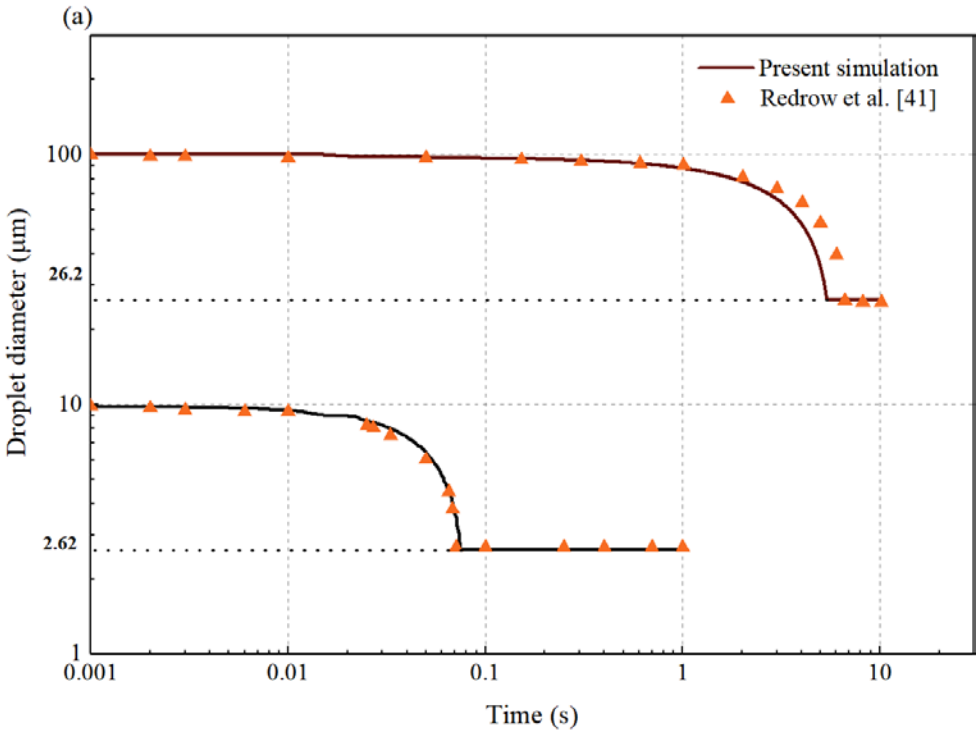

206

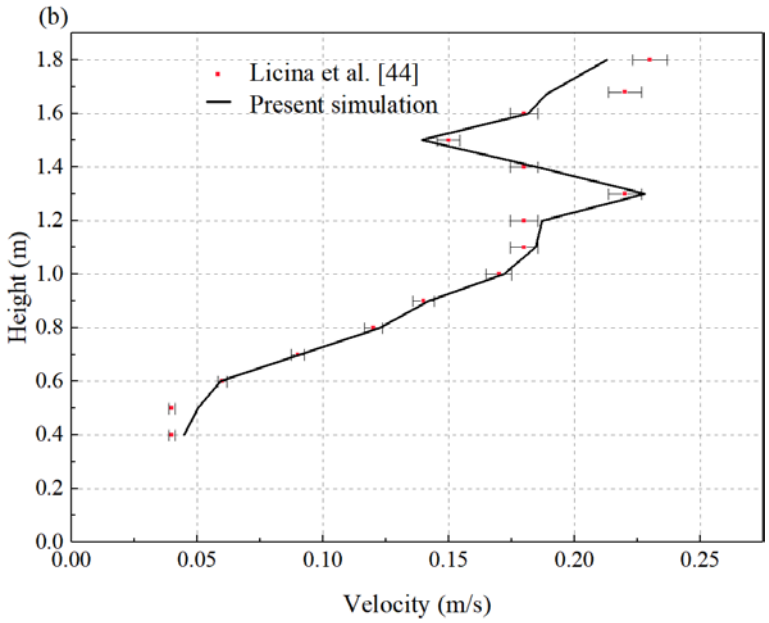

207

208 Figure 4 Numerical model verifications for the discrete and continuous phase models:

209 (a) Evaporation process of the respiratory droplets [41] (b) Human thermal plume

210 characteristics [44]

211

212 # Results

213 ***Evaporation comparison amongst droplet compositions***

Figure 5 presents the evaporation comparison of the initial 100 μm droplet amongst the different investigated cases. The equilibrium size ratio was determined from the evaporation process of single droplets when the volatile compound (water) had been fully dehydrated. The ratio was calculated from the equilibrium size of droplet nuclei divided by the initial droplet size. The difference in the equilibrium sizes and evaporation time was noticed amongst the investigated cases. As for the two-composition droplet models, the equilibrium sizes were: 26.2%, 20.9% and 7.4% of the initial droplet diameter in Case-1, Case-2 and Case-3, respectively. Meanwhile, the equilibrium size ratios for the three-composition droplet model were increased to 41.7%, 21.2% and 11.7% in Cases-4, Case-5 and Casee-6, respectively. The mass fraction distinction in non-volatile components induced the size difference. The size ratio remained constant in the analysis. The results obtained in Case-1 (26.2%) and Case-4 (41.7%) were used to further validate the simulation results. The obtained size ratios were similar to previous studies. [41, 43, 45] As for the evaporation time, three-composition droplet models produced a shorter evaporation time than the two-composition models of the same irrigant type. The longest evaporation time (5.96 s) occurred in the two-composition droplet models diluted with distilled water (Case-3). Considering the differences in the droplet evaporation time and equilibrium size amongst the investigated cases, the droplet propagation and deposition patterns would require further analysis in surgery environments.

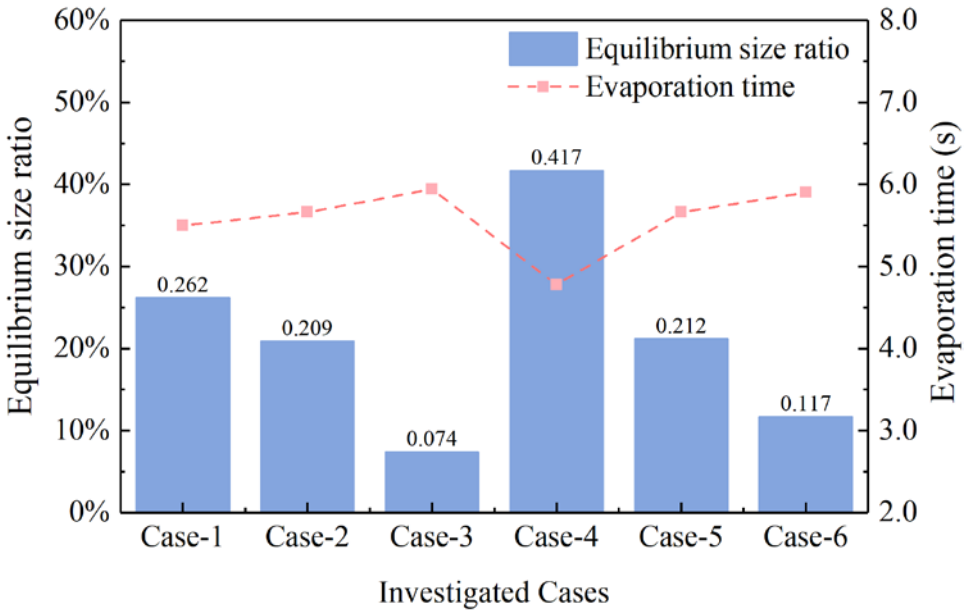

Figure 5 Evaporation comparison of initial 100 μm droplet amongst the different investigated cases: equilibrium size ratio and evaporation time

Airflow patterns in the dental surgery room

Figure 6 demonstrates the velocity vector in the dental surgery room ($Y = 2.04\ m$ plane). The cooling air from the ventilation inlet could move along the ceiling, a phenomenon known as the "Coanda" effect. [46] Airflow separations occurred on the right side of the dental clinic, creating turbulent zones. Airflow mixing was observed between the human thermal plume and the surrounding ventilation flow. Figure 6 (b) illustrates the streamlines in the plane $Z = 1.17\ m$. The airflow velocity was around $0.2\ m/s$. The large vortexes were noted near the dental professional, further promoting the particle deposition. Besides, the recirculation regions near the room walls could further affect the airborne lifetime of suspended particles. Determining the corresponding airborne lifetime was critical to helping the restoration of global dental services. [47]

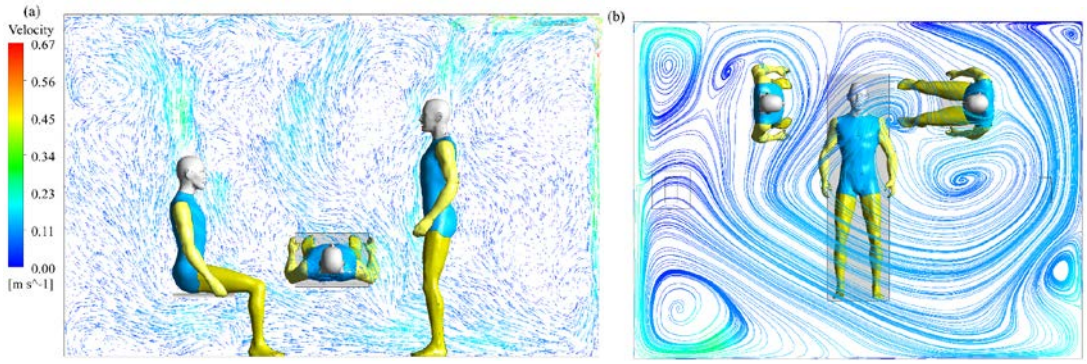

Figure 6 Velocity vector and streamlines in the dental surgery environment: a) $Y = 2.04\ m$ plane and b) $Z = 1.17\ m$ plane, streamlines coloured by the velocity magnitude

Distribution patterns of dental droplets

Figure 7 illustrates the spatial-temporal distribution of dental-emitted droplets in the investigated Case-3, and droplets were coloured based on their diameter. There was no significant difference in the droplet distribution patterns amongst cases. At the initial state of the ultrasonic scaling, $T = 10s$ as shown in Figure 7 (a), droplets would be ejected from the dental treatment region with a high initial momentum. Compared with smaller droplets dehydrated into droplet nuclei, the larger droplets would be directly deposited on the patient's body, dental chair and floor. The trajectories of larger droplets were dominated by gravity. Disinfection in such areas should be focused after the dental procedures. [48] As shown in Figure 7 (b) $T = 1\ min$, some smaller droplets and dehydrated droplet nuclei would be concentrated and move upward. They might be trapped by the room wall and ceiling. The aforementioned propagation patterns could be accounted for by the human thermal plume and surrounding ventilation flow. Besides,

some droplets could concentrate in areas with high turbulent kinetic energy. [32] When gravity was the dominant force for the small droplets, they would depart the cloud and gradually deposit on the ground. As shown in Figure 7 (c) $T = 5\,min$ and (d) $T = 10\,min$, the suspended particles could be transmitted in the entire dental clinic. [10] Some suspended particles would escape through the ventilation exhaust, while others would continue to be suspended in the surgery room. Only a few particles can remain airborne after 20 minutes. Reducing the suspension time and recirculation of small particles in dental clinics can further reduce the fear and uncertainty of possible airborne transmission between appointment patients.

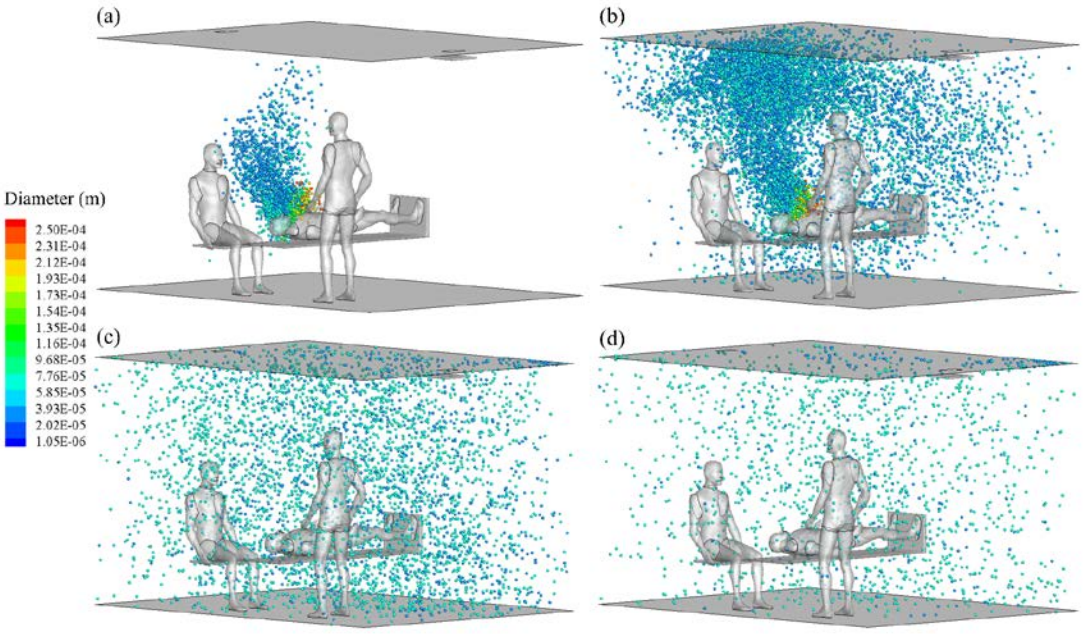

Figure 7 Spatial-temporal distribution of emitted droplets in the investigated Case-3 with the dental irrigant (distilled water): a) $T = 10s$; b) $T = 1\,min$; c) $T = 5\,min$; d) $T = 10\,min$.

The size range of suspended particles presented a significant discrepancy, 5 minutes after the stop of ultrasonic scaling. The size range of suspended particles is presented in Table 2 amongst the investigated cases. The minimum size of suspended particles was in Case-3 (2.0 μm) when distilled water was selected as the dental irrigant. Since the mass fraction of the volatile component (water) in Case-3 droplets was higher than in other cases, the equilibrium size ratio was only 7.4% (referring to Table 1). The maximum size of suspended particles in Case-3 and Case-6 was smaller than 10 μm. The particle size would be trapped in the human upper airways. [49] Dental professionals would be prone to cross-infection if the personal protective equipment is not worn. Besides, the size range of suspended particles in Case-1 and Case-4 (no dilution) was three times that in Case-3 and Case-6 (distilled water). As for Case-2 and Case-5, the use of salt as an adjunct in dental irrigants, as 0.9% normal saline solution, can directly enlarge the size of suspended particles (over 10 μm). The evaporation process would also cause an increase in salt concentration in droplets. The virus viability in droplets can be impacted. [50] As for the organic influence in droplets, all the investigated cases indicated they should not be overlooked. [17] Overall, the mass compositions of the dental liquid mixture can directly affect the size range of suspended particles in dental clinics. The targeted mitigation measures for smaller particle sizes should be developed when using distilled water as the dental irrigant during the atomization procedures.

Table 2 Size range of suspended particles amongst the investigated cases, 5 minutes after the stop of ultrasonic scaling

Case	Minimum size	Maximum size	Size range
Case-1	8.4 μm	15.6 μm	7.2 μm
Case-2	6.8 μm	12.4 μm	5.6 μm
Case-3	2.4 μm	4.4 μm	2.0 μm
Case-4	13.2 μm	24.4 μm	11.2 μm
Case-5	5.7 μm	15.4 μm	9.7 μm
Case-6	3.7 μm	6.8 μm	3.1 μm

Droplet deposition and contamination map

Figure 8 compares the fraction of deposited droplets amongst the investigated cases, 30 minutes after the stop of ultrasonic scaling. When the droplets encountered the human body segments, dental chair, floor and room walls, they would be “trapped” and not be resuspended to the air. When droplets leave the computational domain from the ventilation inlet and outlet, they would no longer be considered in the simulation. The maximum fraction of deposited droplets (88.4%) was found in Case-4 (No dilution), while the minimum (76.2%) was found in Case-3 (distilled water). A higher fraction of deposited droplets was in the three-composition models rather than the two-composition models. Besides, the dental irrigants employed in dental procedures would also impact droplet deposition. Using the 0.9% normal saline (in Case-2 and Case-5) could increase the fraction of deposited droplets by 3% compared with the distilled

water (Case-3 and Case-6). Considering that virus-laden suspended particles would promote long-range airborne transmission, using salt as the adjunct in dental irrigants could help droplet deposition. Figure 8 (b) indicates the detailed droplet deposition map in Case-5, where the droplets were coloured by size. As for the size of the droplets over 50 μm, they would settle on the patient's body. Around 72% of the dental-emitted droplets in the six cases would be deposited on the patient's trunk and head. The composition variation had a small influence on the final deposition. A significant difference in the fraction of deposited droplets was found on dental chairs and floors. It could be accounted for by the discrepancy in the evaporation time and size range of suspended particles. The droplets deposited on the dental professionals' bodies might also promote cross-infection through re-suspension and direct contact.

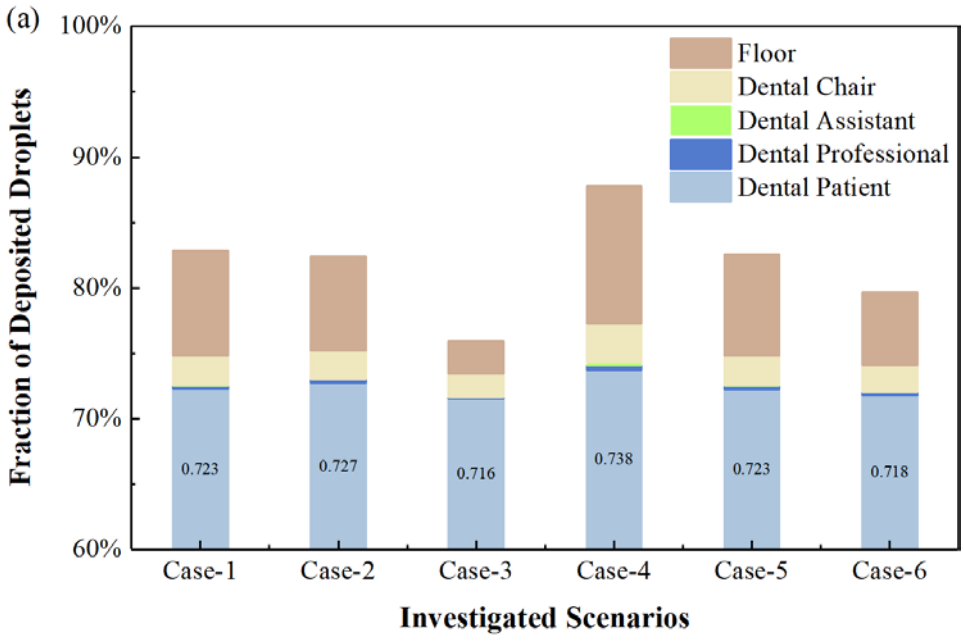

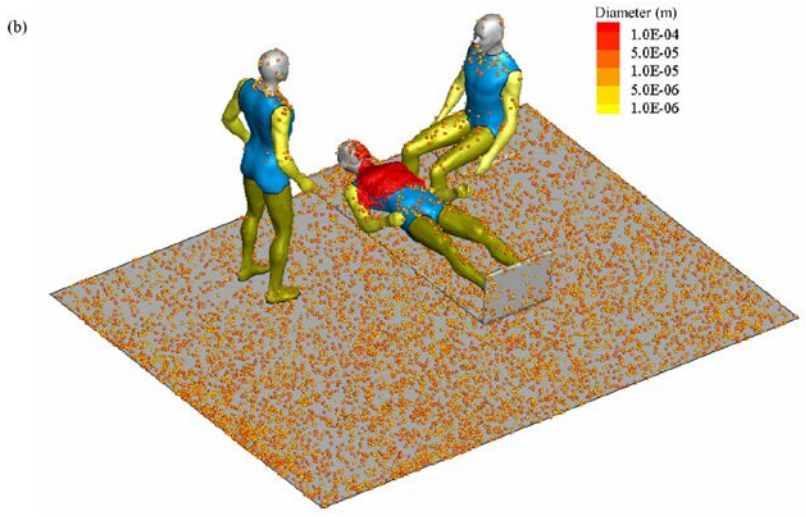

Figure 8 Deposition of dental-emitted droplets, 30 minutes after the stop of ultrasonic scaling: (a) Fraction of deposited droplets amongst the investigated cases (b) droplet deposition map in Case-5 with the coloured droplet size

Discussion and limitations

This study was motivated by the significant concern about influenza and SARS transmission risks in the dental surgery room. In recent decades, several advanced methods have been proposed to investigate the spatial-temporal distribution of particles. [21, 51] Although these image-based techniques can provide some information on the atomization mechanisms of dental procedures, they still lack three-dimensional information about droplet dispersal characteristics. Therefore, CFD simulation was employed in the present study to provide high-resolution results on droplet evaporation, propagation and deposition in dental surgery environments. The results can increase the understanding of the composition effect of dental irrigant and saliva mixture on the characteristics of suspended particles. Source control measures by modifying the rheological properties and compositions of the liquid mixture should be further

recommended in specific dental surgery environments.

The concentration of non-volatile components in droplets can determine the final equilibrium size and evaporation time. However, plenty of research assumed human respiratory droplets as water or inorganic saltine. [7, 33] The simplification above on droplet composition could induce mistakes in cross-infection risk assessments. The virus viability was inversely related to the salt concentration. [50] Droplets emitted from the oral cavity would be subjected to evaporation. It can cause an increase in salt concentrations for around an order of magnitude. [17] Besides, the protein content of respiratory droplets can be elevated by a factor of four when humans are subjected to a respiratory infection. [52] The nonnegligible protein component can potentially impact the phase separation and physical changes in respiratory droplets. Some scholars theoretically found that the droplet composition directly impacted the suspended viral dose. [34] The effect of droplet compositions on the transmission patterns was numerically compared. A much shorter sedimentation time was noticed for the organic-containing droplets. [43] Considering that the studies above were limited to droplets generated during human respiratory activities, the investigation of the effect of droplet composition in the specific dental surgery environment is also warranted. Our present study indicates similar results, with larger deposition rates for the three-composition droplet models in dental surgery.

One type of dental mitigation measure is to use salt and oxidative agents in dental

374 irrigants since such agents can suppress the viability of viruses in droplets. Although
375 some researchers had investigated the effect of viscoelastic properties of the mixture
376 liquid on the atomization mechanism, they did not further specify the difference in the
377 evaporation and propagation properties of droplets. For example, some scholars
378 assessed the effect of H_2O_2 concentrations on dental droplets. [23] They found that
379 adding the oxidant increased the mean droplet size and expelled velocity. The water-
380 based solution of xanthan gum could help reduce droplet generation during dental
381 atomization procedures. [24] While the supply of artificial saliva could increase the
382 generation of larger droplets. [8] The composition of the emitted droplets can be
383 determined by the mixture of human saliva and dental irritants. The deposition and
384 suspension characteristics of the droplets are directly related to their non-volatile
385 components. However, consensus about the composition effect of dental-emitted
386 droplets on their evaporation and propagation patterns has not been well-investigated.
387 Therefore, this study can act as the first research to quantitatively investigate the supply
388 of dental irrigants, as a mitigation measure to suppress the viability of viruses, on
389 droplet evaporation and propagation. In addition, this study also systematically
390 investigated how droplet evaporation patterns can be modified by the interaction of
391 airflow amongst human breathing flow, thermal plume and ambient ventilation flow.
392
393 The present study is limited to the static surgery environment without considering
394 the dental professionals' movement and different ventilation modes, which can further
395 impact the spatial-temporal distribution of dental droplets. Future research would focus

on the impact of dental professionals' interaction and ventilation modes on droplet propagation and evaporation patterns. The relevant droplet composition models are based on the past measurement of human saliva, and the dilution effect of dental irrigants is based on the well-mixed assumption. Using adjunct and non-volatile components in dental unit water may change the rheological properties of the mixture liquid. Future research needs to experimentally visualize the emitted droplet characteristics (size and velocity distribution) cooperating with different types of dental irrigants, further serving as the up-to-date CFD boundary conditions. In addition, the combination of different environmental conditions and droplet composition models should be quantitively investigated in dental surgery environments.

Conclusion

The present study assessed the composition effect of saliva and irrigant mixture on the droplet propagation patterns in dental surgery environments, focusing on droplet spatial-temporal distribution, evaporation and deposition statistics. Modifying the rheological properties and compositions of the dental liquid mixture can act as an effective source control measure during atomization procedures.

Some meaningful conclusions are drawn.

1) Using salt as the adjunct and non-volatile component in distilled water can enlarge the size of suspended particles over 10 μm and increase the fraction of deposited droplets by 3%. After dental atomization procedures, decontamination and

disinfection for all surfaces should be conducted. The size range of suspended particles exhibits an even 300% difference among the irrigant types.

2) Droplets in the three-composition models have shorter evaporation times and larger deposition rates than the two-composition models in the same irrigant type. The organic-containing droplet model should be considered in future relevant research.

Acknowledgments

The work described in this paper was fully supported by a grant from the Research Grants Council of the Hong Kong Special Administrative Region, China (Project No. PolyU 15209723).

Author Contribution

All authors contributed equally in the preparation of this manuscript.

Statements and declarations

The author(s) declared no potential conflicts of interest with respect to the research, authorship, and/or publication of this article.

References

1. Li X, Mak CM, Ma KW and Wong HM. Restoration of dental services after COVID-19: The fallow time determination with laser light scattering. *Sustain Cities Soc* 2021; 74: 103134. DOI: http://doi.org/10.1016/j.scs.2021.103134.
2. Huang JY, Zheng XH, Han L, Wan QJ, Luo DT, Shu ZY, Song CX and Qian H. Evaluating salivary aerosol spread and contamination risks during dental procedures in an open-plan clinic. *J Aerosol Sci* 2024; 179: 106384. DOI: http://doi.org/10.1016/j.jaerosci.2024.106384.

3. Korany HZ, Almhafdy A, Alsaleem SS and Cao SJ. Numerical modelling of ventilation strategies for mitigating cough particles transmission and infection risk in hospital isolation rooms. *Indoor Built Environ* 2024; 33: 957-975. DOI: http://doi.org/10.1177/1420326x241226467.
4. Hu N, Yuan F, Gram A, Yao R and Sadrizadeh S. Review of experimental measurements on particle size distribution and airflow behaviors during human respiration. *Build Environ* 2024; 247: 110994. DOI: http://doi.org/10.1016/j.buildenv.2023.110994.
5. Hu ST, Liu RJ, Li H and Zhu H. Effects of the air temperature on immunoglobulin concentrations of healthy people. *Indoor Built Environ* 2023; 32: 1439-1449. DOI: http://doi.org/10.1177/1420326x231166133.
6. Xu CW, Ren YJ, Li N, Liu L, Mei X and Fan YC. Performance of personalized ventilation in mitigating short-range airborne transmission under the influence of multiple factors. *Build Simul* 2023; 16: 2077-2092. DOI: http://doi.org/10.1007/s12273-023-1035-z.
7. Bu Y, Ooka R, Kikumoto H and Oh W. Recent research on expiratory particles in respiratory viral infection and control strategies: A review. *Sustain Cities Soc* 2021; 73: 103106. DOI: http://doi.org/10.1016/j.scs.2021.103106.
8. Xing C, Ai Z, Liu Z, Mak CM and Wong HM. Characteristics of droplets emission immediately around mouth during dental treatments. *Build Environ* 2024; 248: 111066. DOI: http://doi.org/10.1016/j.buildenv.2023.111066.
9. Li X, Mak CM, Ma KW and Wong HM. Evaluating flow-field and expelled droplets in the mockup dental clinic during the COVID-19 pandemic. *Phys Fluids* 2021; 33: 047111. DOI: http://doi.org/10.1063/5.0048848.
10. Xing CJ, Zhang SS, Bai MH, Ai ZT, Xu CW and Mak CM. Spatiotemporal distribution of aerosols generated by using powder jet handpieces in periodontal department. *Sustain Cities Soc* 2021; 75: 103353. DOI: http://doi.org/10.1016/j.scs.2021.103353.
11. He J, Li J, Chen B, Yang W, Yu X, Zhang F, Li Y, Shu H and Zhu X. Study of aerosol dispersion and control in dental practice. *Clin Oral Investig* 2024; 28: 120. DOI: http://doi.org/10.1007/s00784-024-05524-6.
12. Emery MA, Reed D and McCracken B. Novel use of riboflavin as a fluorescent tracer in the dissemination of aerosol and splatter in an open operatory dental clinic. *Clin Exp Dent Res* 2023; 9: 500-508. DOI: http://doi.org/10.1002/cre2.727.
13. Beltran EO, Castellanos JE, Corredor ZL, Morgado W, Zarta OL, Cortes A, Avila V and Martignon S. Tracing PhiX174 bacteriophage spreading during aerosol-generating procedures in a dental clinic. *Clin Oral Investig* 2023; 27: 3221-3231. DOI: http://doi.org/10.1007/s00784-023-04937-z.
14. Lieber C, Melekidis S, Koch R and Bauer HJ. Insights into the evaporation characteristics of saliva droplets and aerosols: Levitation experiments and numerical modeling. *J Aerosol Sci* 2021; 154: 105760. DOI: http://doi.org/10.1016/j.jaerosci.2021.105760.
15. Liu L, Wei J, Li Y and Ooi A. Evaporation and dispersion of respiratory droplets from coughing. *Indoor Air* 2017; 27: 179-190. DOI: http://doi.org/10.1111/ina.12297.
16. Li X. *A study of pollutant dispersion mechanism in medical environments using particle image velocimetry (PIV) and computational fluid dynamics (CFD)*. Hong Kong Polytechnic University, Hong Kong, 2023.
17. Vejerano EP and Marr LC. Physico-chemical characteristics of evaporating respiratory fluid droplets. *J R Soc Interface* 2018; 15: 20170939. DOI: http://doi.org/10.1098/rsif.2017.0939.
18. Marr LC, Tang JW, Van Mullekom J and Lakdawala SS. Mechanistic insights into the effect of

humidity on airborne influenza virus survival, transmission and incidence. *J R Soc Interface* 2019; 16: 20180298. DOI: http://doi.org/10.1098/rsif.2018.0298.

19. Ra'fat IF. Effect of cooling water temperature on the temperature changes in pulp chamber and at handpiece head during high-speed tooth preparation. *Restorative Dentistry & Endodontics* 2019; 44: DOI: http://doi.org/10.5395/rde.2019.44.e3.

20. Kim MJ, Kuroda M, Kobayashi Y, Yamamoto T, Aizawa T and Satoh K. Visualization of airborne droplets generated with dental handpieces and verification of the efficacy of high-volume evacuators: an in vitro study. *BMC Oral Health* 2023; 23: 976. DOI: http://doi.org/10.1186/s12903-023-03725-1.

21. Kumar MS, He R, Feng L, Olin P, Chew HP, Jardine P, Anderson GC and Hong J. Particle generation and dispersion from high-speed dental drilling. *Clin Oral Investig* 2023; 27: 5439-5448. DOI: http://doi.org/10.1007/s00784-023-05163-3.

22. Li X, Mak CM and Wong HM. Performance of mitigation measures on emitted droplets in dental atomization procedure. In: *E3S Web of Conferences* 2023, p.01046.

23. Roy T, Damoulakis G, Komperda J, Mashayek F, Cooper LF, Rowan SA and Megaridis CM. Effect of H(2)O(2) Antiseptic on Dispersal of Cavitation-Induced Microdroplets. *J Dent Res* 2021; 100: 1258-1264. DOI: http://doi.org/10.1177/00220345211027550.

24. Plog J, Wu J, Dias YJ, Mashayek F, Cooper LF and Yarin AL. Reopening dentistry after COVID-19: Complete suppression of aerosolization in dental procedures by viscoelastic Medusa Gorgo. *Phys Fluids* 2020; 32: 083111. DOI: http://doi.org/10.1063/5.0021476.

25. Li X, Mak CM, Ai ZT, Ma KW and Wong HM. Cross-infection risk assessment in dental clinic: Numerical investigation of emitted droplets during different atomization procedures. *J Build Eng* 2023; 75: 106961. DOI: http://doi.org/10.1016/j.jobe.2023.106961.

26. Li H, Khoa ND, Kuga K and Ito K. In silico identification of viral loads in cough-generated droplets - Seamless integrated analysis of CFPD-HCD-EWF. *Comput Meth Prog Bio* 2024; 246: 108073. DOI: http://doi.org/10.1016/j.cmpb.2024.108073.

27. Abouelhamd I, Kuga K, Yoo SJ and Ito K. Identification of probabilistic size of breathing zone during single inhalation phase in semi-outdoor environmental scenarios. *Build Environ* 2023; 243: 110672. DOI: http://doi.org/10.1016/j.buildenv.2023.110672.

28. Li X, Ai ZT, Ye JJ, Mak CM and Wong HM. Airborne transmission during short-term events: Direct route over indirect route. *Build Simul* 2022; 15: 2097-2110. DOI: http://doi.org/10.1007/s12273-022-0917-9.

29. Dey S, Tunio M, Boryc LC, Hodgson BD and Garcia GJM. Quantifying strategies to minimize aerosol dispersion in dental clinics. *Exp Comput Multiph Flow* 2023; 5: 290-303. DOI: http://doi.org/10.1007/s42757-022-0157-3.

30. Wang L, Wang Z, Zhu S, Zhu Z, Jin T and Wei J. Numerical investigation of impinging jet ventilation in ICUs: Is thermal stratification a problem? *Build Simul* 2023; 16: 1-13. DOI: http://doi.org/10.1007/s12273-023-1023-3.

31. Komperda J, Peyvan A, Li D, Kashir B, Yarin AL, Megaridis CM, Mirbod P, Paprotny I, Cooper LF, Rowan S, Stanford C and Mashayek F. Computer simulation of the SARS-CoV-2 contamination risk in a large dental clinic. *Phys Fluids* 2021; 33: 033328. DOI: http://doi.org/10.1063/5.0043934.

32. Li X, Mak CM, Ai ZT, Ma KW and Wong HM. Numerical investigation of the impacts of environmental conditions and breathing rate on droplet transmission during dental service. *Phys Fluids* 2023; 35:DOI: http://doi.org/10.1063/5.0144647.

33. Khoa ND, Kuga K, Inthavong K and Ito K. Coupled Eulerian Wall Film-Discrete Phase model for

predicting respiratory droplet generation during a coughing event. *Phys Fluids* 2023; 35: DOI: http://doi.org/10.1063/5.0174014.
34. de Oliveira PM, Mesquita LCC, Gkantonas S, Giusti A and Mastorakos E. Evolution of spray and aerosol from respiratory releases: theoretical estimates for insight on viral transmission. *Proc Math Phys Eng Sci* 2021; 477: 20200584. DOI: http://doi.org/10.1098/rspa.2020.0584.
35. Yoo SJ and Ito K. Validation, verification, and quality control of computational fluid dynamics analysis for indoor environments using a computer-simulated person with respiratory tract. *Jpn Archit Rev* 2022; 5: 714-727. DOI: http://doi.org/10.1002/2475-8876.12301.
36. Gupta JK, Lin CH and Chen Q. Characterizing exhaled airflow from breathing and talking. *Indoor Air* 2010; 20: 31-39. DOI: http://doi.org/10.1111/j.1600-0668.2009.00623.x.
37. Li X, Mak CM, Ai ZT and Wong HM. Airborne transmission of exhaled pollutants during short-term events: Quantitatively assessing inhalation monitor points. *Build Environ* 2022; 223: 109487. DOI: http://doi.org/10.1016/j.buildenv.2022.109487.
38. Li X, Mak CM, Ai Z, Ma KW and Wong HM. Propagation and evaporation of contaminated droplets, emission and exposure in surgery environments revealed by laser visualization and numerical characterization. *J Hazard Mater* 2024; 477: 135338. DOI: http://doi.org/10.1016/j.jhazmat.2024.135338.
39. Cunha-Cruz J, Scott J, Rothen M, Mancl L, Lawhorn T, Brossel K, Berg J and Northwest Practice-based RCiE-bD. Salivary characteristics and dental caries: evidence from general dental practices. *J Am Dent Assoc* 2013; 144: e31-40. DOI: http://doi.org/10.14219/jada.archive.2013.0159.
40. ANSYS I. *ANSYS Fluent Theory Guide*. ANSYS, Inc., Canonsburg, PA, 2020.
41. Redrow J, Mao SL, Celik I, Posada JA and Feng ZG. Modeling the evaporation and dispersion of airborne sputum droplets expelled from a human cough. *Build Environ* 2011; 46: 2042-2051. DOI: http://doi.org/10.1016/j.buildenv.2011.04.011.
42. Zhang B, Zhu C, Ji Z and Lin CH. Design and characterization of a cough simulator. *J Breath Res* 2017; 11: 016014. DOI: http://doi.org/10.1088/1752-7163/aa5cc6.
43. Wang TT, Shi FS, Shi FC, Li CH, Zhang L, Wang JB, Jiang C, Qian BS, Dai L and Ji P. Numerical study of the effect of composition models on cough droplet propagation distributions in confined space. *Build Environ* 2023; 234: 110117. DOI: http://doi.org/10.1016/j.buildenv.2023.110117.
44. Licina D, Pantelic J, Melikov A, Sekhar C and Tham KW. Experimental investigation of the human convective boundary layer in a quiescent indoor environment. *Build Environ* 2014; 75: 79-91. DOI: http://doi.org/10.1016/j.buildenv.2014.01.016.
45. Li X, Shang Y, Yan Y, Yang L and Tu J. Modelling of evaporation of cough droplets in inhomogeneous humidity fields using the multi-component Eulerian-Lagrangian approach. *Build Environ* 2018; 128: 68-76. DOI: http://doi.org/10.1016/j.buildenv.2017.11.025.
46. Saadeddin KAR. *The effects of diffuser exit velocity and distance between supply and return apertures on the efficiency of an air distribution system in an office space*. Brookings: South Dakota State University, 2016.
47. Li X, Mak CM, Ai Z, Ma KW and Wong HM. The Airborne Lifetime and Spatial–Temporal Distribution of Emitted Droplets in Dental Procedures. In proceeding of COBEE 2022: the 5th *International Conference on Building Energy and Environment, Concordia University, Montreal, 25th-29th July* 2022, Berlin: Springer, pp.1627-1633.
48. Kratzel A, Steiner S, Todt D, V'Kovski P, Brueggemann Y, Steinmann J, Steinmann E, Thiel V and Pfaender S. Temperature-dependent surface stability of SARS-CoV-2. *J Infect* 2020; 81: 452-482. DOI:

http://doi.org/10.1016/j.jinf.2020.05.074.
49. Fennelly KP. Particle sizes of infectious aerosols: implications for infection control. *Lancet Respir Med* 2020; 8: 914-924. DOI: http://doi.org/10.1016/S2213-2600(20)30323-4.
50. Yang W, Elankumaran S and Marr LC. Relationship between humidity and influenza A viability in droplets and implications for influenza's seasonality. *PLoS One* 2012; 7: e46789. DOI: http://doi.org/10.1371/journal.pone.0046789.
51. Li X, Mak CM, Wai Ma K and Wong HM. How the high-volume evacuation alters the flow-field and particle removal characteristics in the mock-up dental clinic. *Build Environ* 2021; 205: 108225. DOI: http://doi.org/10.1016/j.buildenv.2021.108225.
52. Spicer SS and Martinez JR. Mucin biosynthesis and secretion in the respiratory tract. *Environ Health Perspect* 1984; 55: 193-204. DOI: http://doi.org/10.1289/ehp.8455193.